Received 18 August 2014; revised 21 April 2015; accepted 30 October 2015. Date of publication 8 January 2016;
date of current version 23 March 2016.

*Digital Object Identifier 10.1109/JPETS.2015.2508785*

# Load Model for Medium Voltage Cascaded H-Bridge Multi-Level Inverter Drive Systems

**XIAODONG LIANG[1] (Senior Member, IEEE) AND JINWEI HE[2]**

[1]Department of Electrical and Computer Engineering, Faculty of Engineering and Applied Science, Memorial University of Newfoundland, St. John's, NL A1B 3X9, Canada

[2]School of Electrical Engineering and Automation, Tianjin University, Tianjin 300072, China

CORRESPONDING AUTHOR: X. LIANG (xliang@mun.ca)

**ABSTRACT** Medium voltage drives (MVDs) are commonly used in high-power applications and show significant impact on the overall system dynamics due to their large size and high power demand. Although detailed switching models for MVDs can be built using MATLAB/Simulink, such models cannot be used in large-scale simulation software for power system dynamic studies. To solve this problem, the dynamic load model for the medium voltage cascaded H-bridge multi-level inverter drive and induction motor systems, which is suitable for power system dynamic studies, is proposed in this paper. Analytical formula of the model is presented. The model includes the aggregated effect of an MVD, an induction motor, and their control system, and thus, it can accurately represent the dynamic responses of the motor drive system under disturbances. Both voltage and frequency dependence are considered in the model. The accuracy of the model is verified by a case study. A sensitivity study is conducted to evaluate the impact of the model parameter variation on dynamic response characteristics. The developed load model can be readily inserted in the large-scale power system simulation software for power system dynamic studies.

**INDEX TERMS** Cascaded H-bridge multi-level inverter, frequency dependence, load model, medium voltage drives (MVDs), power system dynamic studies, voltage dependence.

## I. INTRODUCTION

IT HAS been recognized for more than two decades that representations of power system loads for dynamic performance analysis can have significant impact on power system stability. As power systems are designed and operated with a lower stability margin, adequate load models are of major importance [1], [2]. Despite enormous research efforts and acquired knowledge, load modeling remains one of the most uncertain areas in large-scale power system simulations due to the changing nature of loads and the emergence of new types of loads, such as variable frequency drives (VFDs).

VFDs are widely used in various industrial sectors. The modeling needs for such devices become more important as their penetration level in power systems increases over time. Power electronic devices including VFDs were extensively investigated for modeling in the past. Such investigations were mostly focused on the averaged modeling method for converters/rectifiers at the component level [3]–[11]. The dynamic averaged-value model (AVM) of a low-voltage three-phase load commutated converter is proposed in [11] using differential equations. However, the model is only at the converter level, the rest of the components including the DC link, the inverter, the induction motor connected to the inverter output, and the associated control system for the overall motor drive system are not modeled [11].

Although a detailed switching model for a VFD, a motor and their control system can be built using Matlab/Simulink, it cannot be inserted in large scale power system simulation software for power system dynamic studies [5]–[10].

Currently, a capability gap of load modeling for motor drive systems needs to be filled. The IEEE Task Force on Load Representation for Dynamic Performance recommended that a VFD was effectively constant power load if it was able to ride through voltage sags without tripping [1]. However, as indicated in [2], using a constant power load to represent a complex non-linear power electronic device was questionable. Therefore, a proper dynamic modeling method for motor drive systems must be established for power system dynamic studies.

In power systems, a load model is a mathematical representation of the relationship between the bus voltage (magnitude and frequency) and the real and reactive power flowing into the bus; it may refer to the equations themselves or the equations plus specific values for the parameters (e.g., coefficients, exponents) of the equations. There are two types of load models: static and dynamic load models. The static load model involves algebraic equations. It is essentially used for static load components, such as resistive and lighting loads. The dynamic load model involves difference or differential equations [1].

Two types of dynamic load models are proposed for large industrial loads in [12]: a transfer function model, and a composite load model (an induction motor in parallel with a shunt static load). The dynamic load model expressed by a transfer function for power grid is recommended in [13] and [14], which appears to be a well-accepted dynamic load model format.

In an effort to fill the load modeling gap for motor drive systems, References [15] and [16] propose an analytical method called ''linearization approach'' by the lead author. The equivalent load model expressed by transfer functions for a low-voltage drive and an induction motor system is developed in the two papers, and the proposed load modeling method were proved to be effective. In real life, VFDs will trip out of line under large disturbances and will be able to ride-through when experiencing small disturbances. The equivalent load model is intended for the ride-through case related to small disturbances, and thus, it can be treated as a small-signal stability problem. Therefore, the equivalent load model for motor drive systems can be developed using the linearization approach and expressed by transfer functions [15], [16].

Medium voltage drives (MVDs) are commonly used in high power applications and show significant impacts on the overall system dynamics due to their large size and high power demand. Developing adequate dynamic load models for medium voltage motor drive systems is essential for power system stability studies. It is found through extensive literature review that there is no dynamic load model available for medium voltage motor drive systems.

In this paper, a dynamic load model of a medium voltage cascaded H-bridge multi-level inverter drive and an induction motor system is presented. The proposed model is expressed by transfer functions and can be readily used in large scale power system simulation software, such as PSS/E.

The paper is organized as follows: In Section II, the detailed mathematical derivation of the proposed dynamic load model for the medium voltage cascaded H-bridge multi-level inverter motor drive system is presented; the developed dynamic load model is verified by a case study in Section III; In Section IV, a sensitivity study is conducted for the model to evaluate the impact of the model parameter variation on dynamic response characteristics; and, finally, the conclusions are drawn in Section V.

## II. DYNAMIC LOAD MODEL DEVELOPMENT

The medium voltage cascaded H-bridge multi-level inverter drives are one of the topologies for very high power applications [17]–[21]. The drive is constructed using a series of low voltage power modules. Usually, 9 power modules form an 18-pulse system, and 12 power modules form a 24-pulse system at the drive input. The topology of a 9-power-module 18-pulse medium voltage drive can be found in [17] and [19]. For these 18-pulse drives, there are three power modules in a phase leg, and the drives can produce as much as 1,440 V line-to-neutral, or 2,494 V line-to-line at the output. The topology of a nine-power-module 18-pulse medium voltage drive and an induction motor system is shown in Fig. 1(a). Similarly, for 24-pulse drives with four power modules in a phase leg, the drives can produce line-to-neutral voltage up to 1,920 V (line-to-line voltage up to 3,325 V). At the drive input, there is a phase-shifting transformer. The phase-shift angle differs by multiples of 20° for 18-pulse drives and by multiples of 15° for 24-pulse drives [17].

Each power module is a static pulse-width-modulated (PWM) power converter. It consists of a three-phase full bridge diode converter, a DC link, and a single-phase full bridge inverter. The schematic diagram of each power module is shown in Fig. 1(b). The three-phase full bridge diode converter is exactly the same as the low voltage 6-pulse drive, which is capable of receiving input power from one of the phase-shifting transformer secondary windings at 480 V, 50/60 Hz, and charging a DC link capacitor to about 600 V dc voltage. The DC voltage feeds a single-phase full bridge inverter, which is delivered to a single-phase load at any voltage up to 480 V [17]. The outputs of multiple single-phase inverters are connected in series, feeding one phase of an induction motor [20]. The outputs of the single-phase full bridge inverters connected to phase a of an induction motor are shown in Fig. 1(c).

### A. MATHEMATICAL MODEL OF CONVERTER AND DC LINK FOR EACH POWER MODULE AND INDUCTION MOTOR

In this paper, the mathematical derivation of the dynamic load model for a medium voltage cascaded H-bridge multi-level inverter motor drive system starts from each low voltage power module.

For the low voltage power modules connected to the transformer secondary windings without a phase-shifting (i.e., the phase-shifting angle is equal to 0°), differential equations for the converter and the DC link are the same as that used for the low-voltage voltage source inverter drive in [15] and [16]. Similarly, differential equations of induction motors can be found in [15], [16], [22], and [23]. Therefore, these equations will not be repeated in the paper.

### B. MATHEMATICAL MODEL OF THE INVERTER FOR EACH POWER MODULE

It is verified in this study that the DC link voltage from the diode converter connected to the transformer secondary winding with a phase-shifting angle not equal to 0° are exactly the same as that from the diode converter connected to the transformer secondary winding with

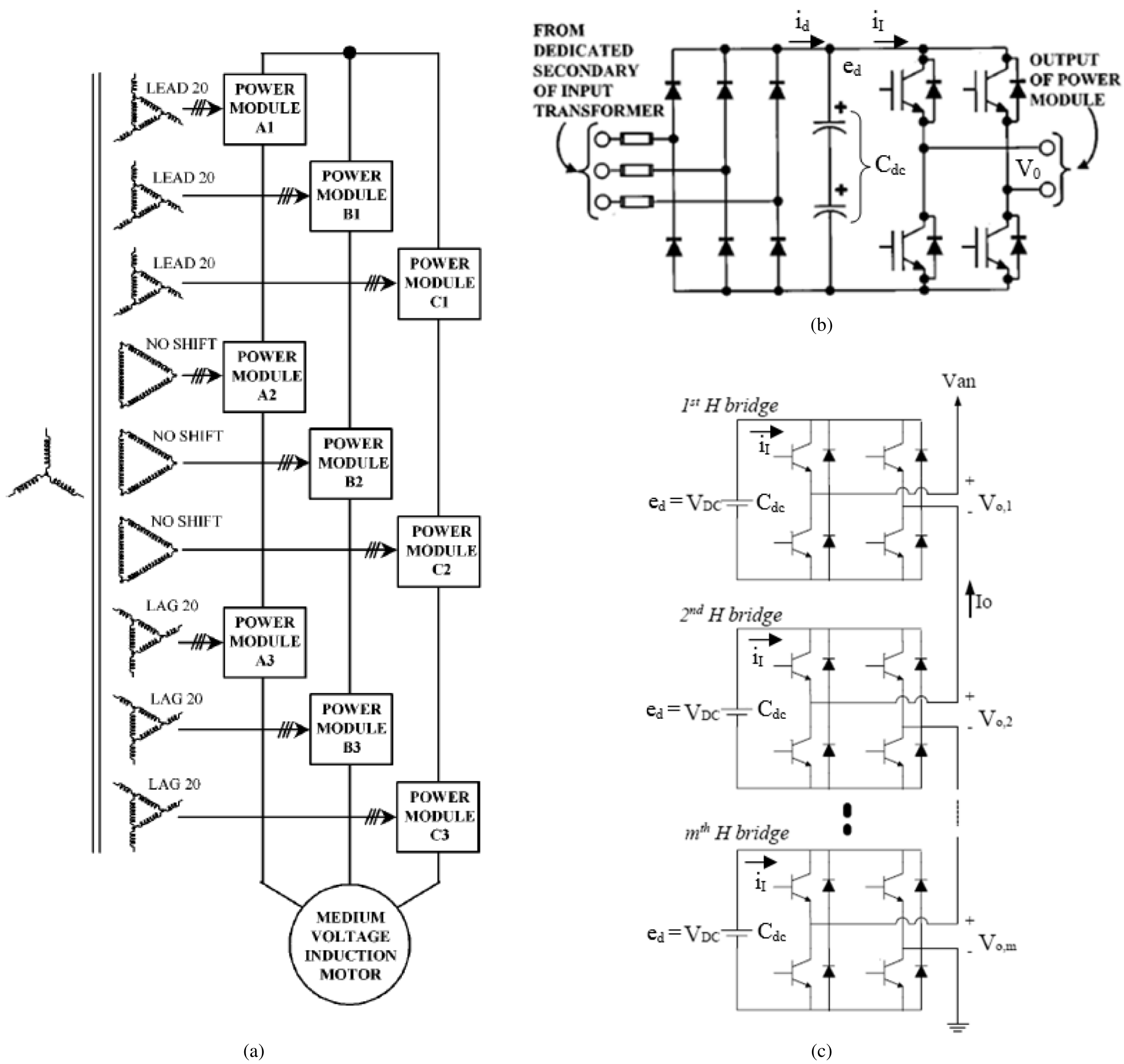


**FIGURE 1. Eighteen-pulse cascaded H-bridge multi-level inverter motor drive system: (a) the topology of a nine-power-module drive [17]; (b) the schematic diagram for each power module [17]; (c) outputs of the single-phase full bridge inverters connected to phase a of an induction motor [20].**

a phase-shifting angle equal to 0°. Therefore, the phase shift angle of the transformer winding does not affect the DC link voltage from the converter in each power module.

The output voltage from the single-phase full bridge inverter for each power module can be determined as follows:

$$V_0 = de_d \tag{1}$$

where $V_0$ is the output voltage from each power module, $d$ is duty cycle, $e_d$ is the DC link voltage before the inverter.

The line to neutral voltage of the induction motor at phase $aV_{an}$ can be determined as follows:

$$V_{an} = \left(\frac{n_{pulse}}{6}\right) de_d \cos(\omega_s t) \tag{2}$$

where, $n_{pulse}$ is the pulse number of the medium voltage drive, $\omega_s$ is the stator electrical field angular velocity in rad/s for the induction motor.

For an 18-pulse medium voltage drive, three power modules per phase are connected to the induction motor. The pulse number $n_{pulse}$ is assigned as follows:

$$n_{pulse} = 18. \tag{3}$$

The voltages at phases $b$ and $c$ can be determined similarly as phase a by the following equations:

$$V_{bn} = \left(\frac{n_{pulse}}{6}\right) de_d \cos\left(\omega_s t - \frac{2\pi}{3}\right) \tag{4}$$

$$V_{cn} = \left(\frac{n_{pulse}}{6}\right) de_d \cos\left(\omega_s t + \frac{2\pi}{3}\right). \tag{5}$$

The three phase line-to-neutral voltages of the induction motor in the *abc* frame are converted to the *dq0* frame by

$$V_{qs} = \left(\frac{n_{pulse}}{6}\right) de_d \tag{6}$$

$$V_{ds} = 0 \tag{7}$$

where $v_{qs}$ is the q-axis voltage at the terminal of the induction motor, and $v_{ds}$ is the d-axis voltage at the terminal of the induction motor.

The real power supplied to the induction motor $P_{ac\_IM}$ can be expressed as follows:

$$\begin{aligned} P_{ac\_IM} &= \frac{3}{2}\left(V_{ds}i_{qs} + V_{qs}i_{qs}\right) = \frac{3}{2}V_{qs}i_{qs} \\ &= \frac{3}{2} \times \left(\frac{n_{pulse}}{6}de_d\right) i_{qs} = \left(\frac{n_{pulse}}{4}\right) de_d i_{qs} \end{aligned} \tag{8}$$

where $i_{ds}$ and $i_{qs}$ are the d- and q-axis components of the stator current of the induction motor, respectively.

The total DC power at the DC link for all power modules, $P_{dc}$, corresponding to the real power supplied to the induction motor can be calculated as follows:

$$P_{dc} = \left(\frac{n_{pulse}}{2}\right) P_{dc\_\text{per module}} = \left(\frac{n_{pulse}}{2}\right) e_d i_I \tag{9}$$

where, $i_I$ is the DC link current entering the inverter inside each power module.

Ignoring losses at the inverters inside power modules, the following equation is satisfied:

$$P_{ac\_IM} = P_{dc}. \tag{10}$$

Based on (8)-(10), we have

$$\left(\frac{n_{pulse}}{4}\right) de_d i_{qs} = \left(\frac{n_{pulse}}{2}\right) e_d i_I. \tag{11}$$

The DC link current entering the inverter $i_I$, the DC link current after the converter/rectifier $i_d$, the DC link voltage before the inverter $e_d$, and the capacitance of the DC link capacitor $C_{dc}$ have the following relationship:

$$i_I = i_d - C_{dc}\frac{de_d}{dt}. \tag{12}$$

Substitute (12) in (11), we have

$$\frac{1}{2}de_d i_{qs} = e_d\left(i_d - C_{dc}\frac{de_d}{dt}\right). \tag{13}$$

The q-axis component of the motor stator current can be determined from (13) as follows:

$$i_{qs} = \frac{2i_d}{d} - 2C_{dc}\left(\frac{de_d}{dt}\frac{1}{d}\right). \tag{14}$$

Linearize (14), the following can be determined:

$$\Delta i_{qs} = \frac{2}{d_0}\Delta i_d - \frac{i_{qs0}}{d_0}\Delta d - \frac{2C_{dc}}{d_0}S\Delta e_d \tag{15}$$

where S is the Laplace Transform variable.

### *C. MATHEMATICAL MODEL OF THE CONTROL SCHEME*

The control system used in load modeling of the medium voltage motor drive system is the closed-loop voltage per Hz control. If a different control method is used, equations for control systems need to be adjusted accordingly. Reference [11] provides information on the voltage control method for the duty-cycle modulator. The goal is to obtain the appropriate duty cycle(s) and the converter reference frame position in order to achieve a desired fast average synchronous reference frame direct- and quadrature-axis voltages [11].

The voltage command related to the duty-cycle modulation can be expressed as follows [11]:

$$\begin{bmatrix} v_{qs}^e \\ v_{ds}^e \end{bmatrix} = \begin{bmatrix} \cos\theta_{ce} & \sin\theta_{ce} \\ -\sin\theta_{ce} & \cos\theta_{ce} \end{bmatrix}\begin{bmatrix} v_{qs}^c \\ v_{ds}^c \end{bmatrix} \tag{16}$$

where $\theta_{\text{ce}}$ is angular displacement of the converter reference frame from the synchronous reference frame, and

$$\theta_{ce} = \theta_c - \theta_e. \tag{17}$$

In this research work, the sine-triangle PWM is considered. Replacing $v_{qs}^e$ with the commanded value $v_{qs}^{e*}$, replacing $v_{ds}^e$ with the commanded value $v_{ds}^{e*}$, and replacing $v_{qs}^c$ and $v_{ds}^c$ with the average values expression by (6) and (7) yield

$$\begin{aligned} \begin{bmatrix} v_{qs}^{e*} \\ v_{ds}^{e*} \end{bmatrix} &= \begin{bmatrix} \cos\theta_{ce} & \sin\theta_{ce} \\ -\sin\theta_{ce} & \cos\theta_{ce} \end{bmatrix}\begin{bmatrix} v_{qs} \\ v_{ds} \end{bmatrix} \\ &= \begin{bmatrix} \cos\theta_{ce} & \sin\theta_{ce} \\ -\sin\theta_{ce} & \cos\theta_{ce} \end{bmatrix}\begin{bmatrix} \frac{n_{pulse}}{6}de_d \\ 0 \end{bmatrix}. \end{aligned} \tag{18}$$

From (18), the following relationships are obtained:

$$d = \frac{\sqrt{\left(v_{qs}^{e*}\right)^2 + \left(v_{ds}^{e*}\right)^2}}{\left(\frac{n_{pulse}}{6}\right)e_d}. \tag{19}$$

The block diagram for the closed-loop voltage per Hz control scheme used in this study is shown in Fig. 2. The equations for the closed-loop voltage per Hz control are given as follows:

$$\begin{aligned} \omega_{SL} &= K_{pm}\left(\omega_r^* - \omega_r\right) + \int_0^t K_{im}\left(\omega_r^* - \omega_r\right)dt \\ &\quad + \left(\omega_{s0} - \omega_{r0}\right) \end{aligned} \tag{20}$$

$$\omega_{SL} + \omega_r = \omega_s \tag{21}$$

$$d = \frac{\omega_s\left(\frac{V_b}{\omega_b}\right)\sqrt{2}}{\left(\frac{n_{pulse}}{6}\right)e_d} \tag{22}$$

$$V_{qs}^{e*} = \omega_s\left(\frac{V_b}{\omega_b}\right)\sqrt{2} \tag{23}$$

$$V_{ds}^{e*} = 0 \tag{24}$$

where, $K_{pm}$ is speed proportional-integral (*PI*) controller proportional gain; $K_{im}$ is speed *PI* controller integral gain;

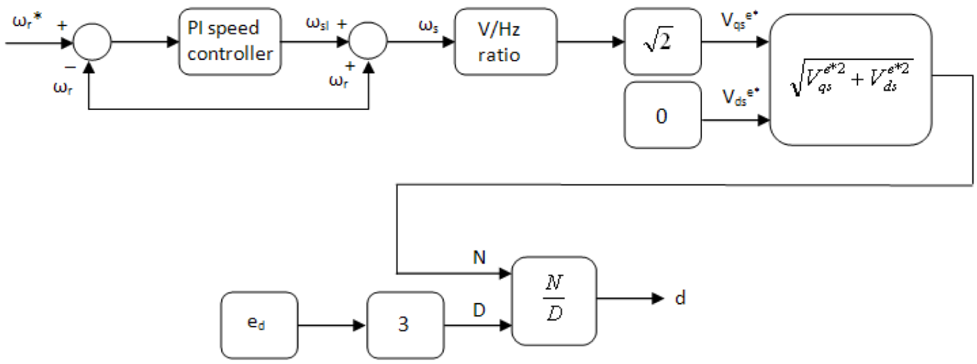


**FIGURE 2.** **Closed-loop voltage per Hz control scheme for the 18-pulse cascaded H-bridge multi-level inverter motor drive system.**

$V_b$ is the nominal voltage of the motor per phase; $\omega_r$ is the electric angular velocity of the rotor in rad/s for the induction motor; $\omega_{SL}$ is the slip angular velocity of the rotor in rad/s. The parameters with a star as the superscript are reference parameters, and with 0 as the subscript are initial values.

Linearize (20) and (21), the relationship between $\omega_s$ and $\omega_r$ can be determined as follows:

$$\Delta\omega_s = \frac{A_{11}S + A_{12}}{S}\Delta\omega_r \tag{25}$$
$$A_{11} = 1 - K_{pm} \tag{26}$$
$$A_{12} = -K_{im}. \tag{27}$$

Linearize (22)

$$\Delta d = \left(-\frac{\sqrt{2}V_b\omega_{s0}}{\frac{n_{pulse}}{6}\omega_b e_{d0}^2}\right)\Delta e_d + \left(\frac{\sqrt{2}V_b}{\frac{n_{pulse}}{6}\omega_b e_{d0}}\right)\Delta\omega_s. \tag{28}$$

Substitute (28) in (15)

$$\Delta i_{qs} = A_{21}\Delta i_d + A_{22}\Delta\omega_s + (A_{231}S + A_{232})\Delta e_d \tag{29}$$
$$A_{21} = \frac{2}{d_0} \tag{30}$$
$$A_{22} = -\frac{\sqrt{2}i_{qs0}V_b}{\frac{n_{pulse}}{6}d_0\omega_b e_{d0}} \tag{31}$$
$$A_{231} = -\frac{2C_{dc}}{d_0} \tag{32}$$
$$A_{232} = \frac{\sqrt{2}i_{qs0}V_b\omega_{s0}}{\frac{n_{pulse}}{6}d_0\omega_b e_{d0}^2}. \tag{33}$$

Linearize (6)

$$\Delta V_{qs} = \left(\frac{n_{pulse}}{6}\right)d_0\Delta e_d + \left(\frac{n_{pulse}}{6}\right)e_{d0}\Delta d. \tag{34}$$

**TABLE 1.** **Electrical parameters of the sample motor drive system (required input data for Matlab programming).**

| Induction Motor Parameters | Converter, inverter, DC parameters, PI speed controller |
|---|---|
| Nominal power 1500 HP<br>Nominal voltage $V_b$ = 2300 V (rms)<br>Nominal frequency $f_{rated}$ = 60 Hz<br>$R_s$ = 0.056 Ω, $l_s$ = 0.001 H<br>$R_r$ = 0.037 Ω, $l_r$ = 0.001 H<br>$L_m$ = 0.0527 H<br>Inertia J = 44.548 Kg* $m^2$<br>Nominal speed $n_{nom}$ = 1783 rpm<br>Pole pairs p = 2<br>Load torque $T_L$ = 1500 Nm<br>Target speed $n_{oper}$ = 1771 rpm | Diode forward voltage $V_{diode}$ = 1.3 V<br>DC bus capacitor $C_{dc}$ = 10000e-6 F<br>DC bus resistance $r_{dc}$ = 0 Ω<br>DC bus inductance $L_{dc}$ = 0 H<br>Output frequency $f_{out}$ = 60 Hz<br>PI speed controller Proportional gain $K_{pm}$ = 9<br>PI speed controller Integral gain $K_{im}$ = 10 |
| Power Source | |
| Rated voltage 480 V (rms)<br>Rated frequency $f_g$ = 60 Hz<br>Commutation inductance $l_c$ including the phase-shifting transformer impedance = 1.2 mH | |

Substitute (28) in (34), we have

$$\begin{aligned}\Delta V_{qs} &= \left(\frac{n_{pulse}}{6}\right)d_0\Delta e_d + \left(\frac{n_{pulse}}{6}e_{d0}\right)\\ &\quad\times\left(-\frac{\sqrt{2}V_b\omega_{s0}}{\frac{n_{pulse}}{6}\omega_b e_{d0}^2}\Delta e_d + \frac{\sqrt{2}V_b}{\frac{n_{pulse}}{6}\omega_b e_{d0}}\Delta\omega_s\right)\\ &= A_{31}\Delta\omega_s + A_{32}\Delta e_d \end{aligned}\tag{35}$$
$$A_{31} = \frac{\sqrt{2}V_b}{\omega_b} \tag{36}$$
$$A_{32} = \frac{n_{pulse}}{6}d_0 - \frac{\sqrt{2}V_b\omega_{s0}}{\omega_b e_{d0}}. \tag{37}$$

### *D. THE DERIVED DYNAMIC LOAD MODEL FOR THE MOTOR DRIVE SYSTEM*

At the input of the drive, the real and reactive power at each power module are the same, and thus, the total real power ($P_{ac}$) and reactive power ($Q_{ac}$) can be expressed by the power module number, $\frac{n_{pulse}}{2}$, multiplied by the real and reactive power for each power module as follows (for exam-

**TABLE 2. Calculated dynamic load model for the sample 18-pulse medium voltage motor drive system.**

| | |
|---|---|
| $P_0 = 291$ kW, $Q_0 = 73$ kVAR | |
| $G_{P1} =$ | $\dfrac{0.0388\,S^7 + 203.1771\,S^6 + 3.9584\times10^4 S^5 + 9.4318\times10^5 S^4 + 3.2896\times10^7 S^3 + 2.6099\times10^8 S^2 + 1.3533\times10^9 S + 8.0349\times10^8}{-3.5641\times10^{-5} S^7 - 0.0133\,S^6 - 2.8328\,S^5 - 347.3130\,S^4 - 1.2962\times10^4 S^3 - 3.8931\times10^5 S^2 - 4.6363\times10^6 S - 4.819\times10^6}$ |
| $G_{P2} =$ | $\dfrac{7.2285\times10^{-6} S^7 + 0.6836\,S^6 + 132.2883\,S^5 + 2.1104\times10^3 S^4 + 7.0446\times10^4 S^3 - 5.0765\times10^5 S^2 - 1.2378\times10^7 S - 1.5042\times10^7}{-3.5641\times10^{-5} S^7 - 0.0133\,S^6 - 2.8328\,S^5 - 347.3130\,S^4 - 1.2962\times10^4 S^3 - 3.8931\times10^5 S^2 - 4.6363\times10^6 S - 4.819\times10^6}$ |
| $G_{P3} =$ | $\dfrac{-0.0062\,S^7 - 32.3206\,S^6 - 6.2968\times10^3 S^5 - 1.5004\times10^5 S^4 - 5.2329\times10^6 S^3 - 4.1517\times10^7 S^2 - 2.1528\times10^8 S - 1.2782\times10^8}{-3.5641\times10^{-5} S^7 - 0.0133\,S^6 - 2.8328\,S^5 - 347.3130\,S^4 - 1.2962\times10^4 S^3 - 3.8931\times10^5 S^2 - 4.6363\times10^6 S - 4.819\times10^6}$ |
| $G_{P4} =$ | $\dfrac{-2.2258\times10^{-5} S^7 - 0.1166\,S^6 - 22.7216\,S^5 - 541.3991\,S^4 - 1.8883\times10^4 S^3 - 1.4981\times10^5 S^2 - 7.7682\times10^5 S - 4.6122\times10^5}{-3.5641\times10^{-5} S^7 - 0.0133\,S^6 - 2.8328\,S^5 - 347.3130\,S^4 - 1.2962\times10^4 S^3 - 3.8931\times10^5 S^2 - 4.6363\times10^6 S - 4.819\times10^6}$ |
| $G_{Q1} =$ | $\dfrac{0.0048\,S^7 + 75.7226\,S^6 + 1.4683\times10^4 S^5 + 2.6868\times10^5 S^4 + 9.1246\times10^6 S^3 - 1.0722\times10^7 S^2 - 8.1504\times10^8 S - 1.0834\times10^9}{-3.5641\times10^{-5} S^7 - 0.0133\,S^6 - 2.8328\,S^5 - 347.3130\,S^4 - 1.2962\times10^4 S^3 - 3.8931\times10^5 S^2 - 4.6363\times10^6 S - 4.819\times10^6}$ |
| $G_{Q2} =$ | $\dfrac{-2.5154\times10^{-5} S^7 + 0.2573\,S^6 + 49.5929\,S^5 + 553.9201\,S^4 + 1.7416\times10^4 S^3 - 5.0453\times10^5 S^2 - 8.4886\times10^6 S - 9.6756\times10^6}{-3.5641\times10^{-5} S^7 - 0.0133\,S^6 - 2.8328\,S^5 - 347.3130\,S^4 - 1.2962\times10^4 S^3 - 3.8931\times10^5 S^2 - 4.6363\times10^6 S - 4.819\times10^6}$ |
| $G_{Q3} =$ | $\dfrac{0.0215\,S^7 - 3.7420\,S^6 - 568.3827\,S^5 + 1.7394\times10^5 S^4 + 6.6348\times10^6 S^3 + 2.4459\times10^8 S^2 + 3.0221\times10^9 S + 3.1788\times10^9}{-3.5641\times10^{-5} S^7 - 0.0133\,S^6 - 2.8328\,S^5 - 347.3130\,S^4 - 1.2962\times10^4 S^3 - 3.8931\times10^5 S^2 - 4.6363\times10^6 S - 4.819\times10^6}$ |
| $G_{Q4} =$ | $\dfrac{7.7453\times10^{-5} S^7 - 0.0135\,S^6 - 2.0510\,S^5 + 627.6462\,S^4 + 2.3941\times10^4 S^3 + 8.8257\times10^5 S^2 + 1.0905\times10^7 S + 1.1470\times10^7}{-3.5641\times10^{-5} S^7 - 0.0133\,S^6 - 2.8328\,S^5 - 347.3130\,S^4 - 1.2962\times10^4 S^3 - 3.8931\times10^5 S^2 - 4.6363\times10^6 S - 4.819\times10^6}$ |

ple, for an 18-pulse drive, the power module number is 9):

$$P_{ac} = \left(\frac{n_{pulse}}{2}\right) P_{ac\_per\,\mathrm{mod}\,ule} \tag{38}$$

$$Q_{ac} = \left(\frac{n_{pulse}}{2}\right) Q_{ac\_per\,\mathrm{mod}\,ule} \tag{39}$$

$$P_{ac\_per\,\mathrm{mod}\,ule} = \frac{3}{2}\left(V_{dg} i_{dg} + V_{qg} i_{qg}\right) \tag{40}$$

$$Q_{ac\_per\,\mathrm{mod}\,ule} = \frac{3}{2}\left(-V_{dg} i_{qg} + V_{qg} i_{dg}\right) \tag{41}$$

$$V_{qg} = \sqrt{2}E \tag{42}$$

$$V_{dg} = 0 \tag{43}$$

where, $V_{dg}$ and $V_{qg}$ are d- and q-axis power source voltage per phase at the input of each power module.

By combining differential equations of the converter, the DC link, the inverter, the induction motor and the control system, and conducting linearization for the whole set of differential equations of the overall system, the equivalent dynamic model for the medium voltage motor system is obtained as follows:

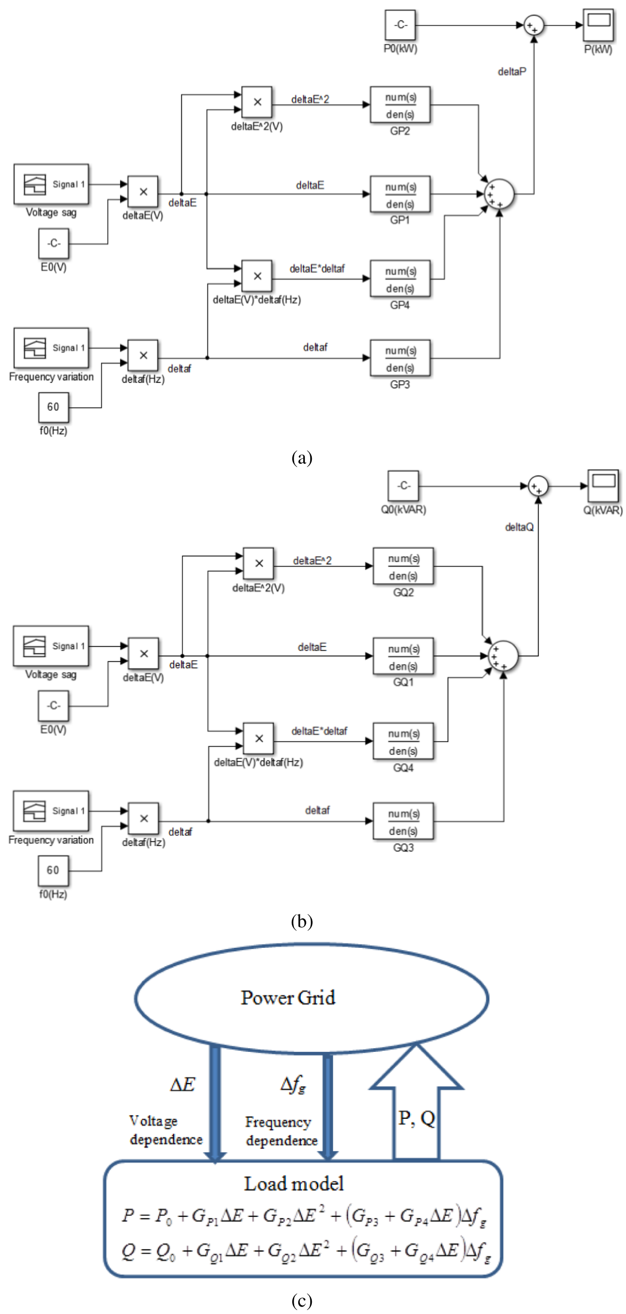


**FIGURE 3. Simulink model and its schematic diagram based on the developed model for the sample system: (a) Simulink model for the real power P; (b) Simulink model for the reactive power Q; and (c) schematic diagram of the developed load model and the power grid simulation studies.**

$$P = P_0 + G_{P1}\Delta E + G_{P2}\Delta E^2 + (G_{P3} + G_{P4}\Delta E)\Delta f_g \tag{44}$$

$$Q = Q_0 + G_{Q1}\Delta E + G_{Q2}\Delta E^2 + (G_{Q3} + G_{Q4}\Delta E)\Delta f_g. \tag{45}$$

The coefficients ($G_{Pi}$, $G_{Qi}$, $i = 1, 2, 3, 4$) in (44)-(45) are the 7th order transfer functions. The proposed dynamic model is expressed by these coefficients. Both voltage and frequency

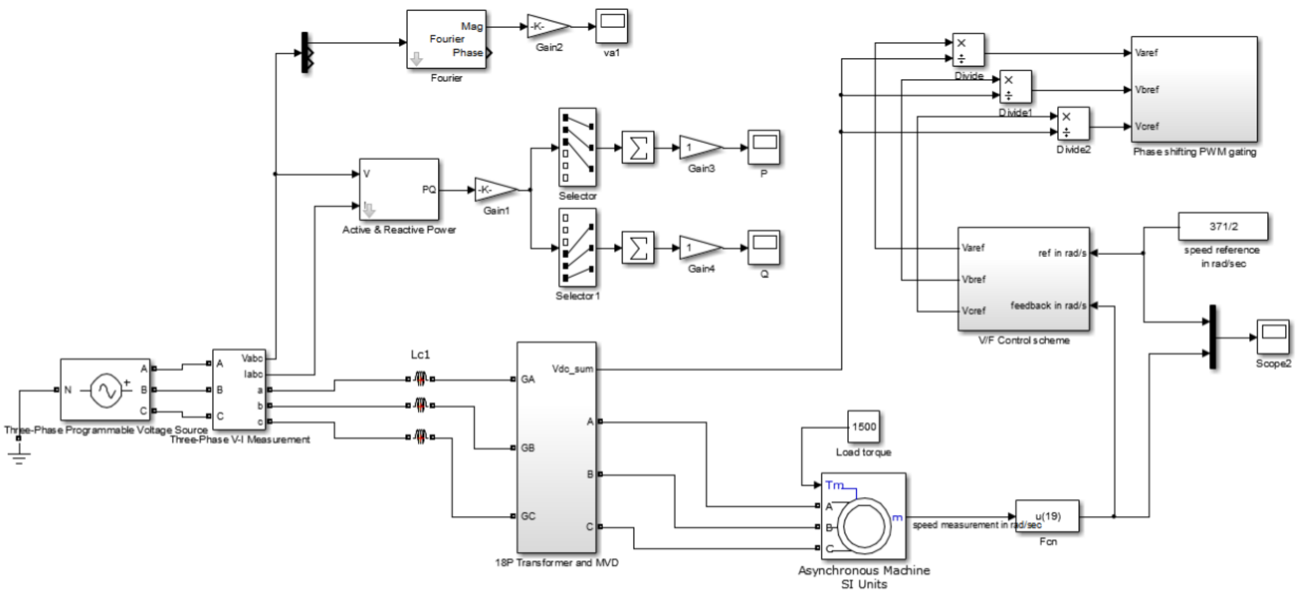


FIGURE 4. **Detailed switching model for the sample system built using Simulink.**

dependence are considered in these coefficients

$$G_{Pi} = \frac{\begin{pmatrix} GP_{i1}S^7 + GP_{i2}S^6 + GP_{i3}S^5 + GP_{i4}S^4 + \\ GP_{i5}S^3 + GP_{i6}S^2 + GP_{i7}S + G_{i8} \end{pmatrix}}{\begin{pmatrix} P_{b1}S^7 + P_{b2}S^6 + P_{b3}S^5 + P_{b4}S^4 + \\ P_{b5}S^3 + P_{b6}S^2 + P_{b7}S + P_{b8} \end{pmatrix}} \quad (i = 1,\ 2,\ 3,\ 4) \tag{46}$$

$$G_{Qi} = \frac{\begin{pmatrix} GQ_{i1}S^7 + GQ_{i2}S^6 + GQ_{i3}S^5 + GQ_{i4}S^4 + \\ GQ_{i5}S^3 + GQ_{i6}S^2 + GQ_{i7}S + GQ_{i8} \end{pmatrix}}{\begin{pmatrix} P_{b1}S^7 + P_{b2}S^6 + P_{b3}S^5 + P_{b4}S^4 + \\ P_{b5}S^3 + P_{b6}S^2 + P_{b7}S + P_{b8} \end{pmatrix}} \quad (i = 1,\ 2,\ 3,\ 4) \tag{47}$$

$$\Delta E = E - E_0 \tag{48}$$

$$\Delta f_g = f_g - f_{g0} \tag{49}$$

where, $P_0$ and $Q_0$ are the initial real and reactive power, $E_0$ is the initial voltage per phase, $f_{g0}$ is the initial frequency at AC input side of the drive connecting to the power grid. The parameters used to calculate the eight coefficients, $G_{Pi1}$–$G_{Pi8}$, $G_{Qi1}$–$G_{Qi8}$, $i$ = 1, 2, 3, 4, and $P_{b1}$–$P_{b8}$, are real constant numbers for a given drive system, these values are determined by parameters involved in all differential equations. S is the Laplace transform variable. For a given system, the denominators of the transfer functions for all coefficients appear to be the same, which are calculated by $P_{b1}$–$P_{b8}$.

Due to page limits of the paper, it is difficult to show the complete derivation process and illustrate each individual parameter involved during such a derivation process. However, the derived dynamic load model includes the aggregated effect of all parameters in these equations. The derived model is generic for this type of motor drive systems, and can be used for drives with different pulse numbers at the input. For example, for an 18-pulse or a 24-pulse drive, just simply assign the pulse number $n_{pulse}$ in (3) as 18 or 24 accordingly.

The whole mathematical derivation was translated into a Matlab program. The required parameters are listed as the input data in the Matlab programming code, and the output data of the Matlab program are the coefficients ($G_{Pi}$, $G_{Qi}$, $i$ = 1, 2, 3, 4). The Matlab program will be used to calculate the specific dynamic model for a given motor drive system.

The proposed modeling concept in the medium voltage motor drive systems can be used for large induction motor or synchronous motor applications. If it is a synchronous motor, differential equations for synchronous machines should be used in Section II-A to derive the dynamic load model.

## III. VERIFICATION OF THE DEVELOPED DYNAMIC LOAD MODEL USING A CASE STUDY

### *A. THE SAMPLE SYSTEM*

A case study is conducted using a sample medium voltage cascaded H-bridge multi-level PWM inverter motor drive system to verify the developed model. The calculated model using the proposed method will be compared with a detailed switching model. A detailed switching model built using Matlab/Simulink for power electronic devices is widely accepted in the circuit design and analysis, therefore, such a model can serve as a form of verification for the developed dynamic load model.

The sample system consists of an 18-pulse medium voltage cascaded H-bridge multi-level voltage source inverter drive, and an induction motor rated at 2300 V and 1500 HP. The control scheme is the closed-loop voltage per Hz control. The parameters of the sample system are shown in Table I, they are also the required input data for the Matlab program. Although the mathematical derivation involves many differential equations, the required input data using the proposed method are quite simple. The output data of the Matlab program for the sample system are calculated as shown in Table II, where the calculated coefficients forming the derived dynamic load model for this particular motor drive system are illustrated. The coefficients are 7$^{th}$ order transfer functions.

The calculated dynamic load model considers both voltage and frequency dependence ($\Delta E$ and $\Delta f_g$). To verify this model, two simulation models for the same sample system are created using Matlab/Simulink: one is the calculated load model [Fig. 3(a) and (b)], another is the detailed switching model (Fig. 4). Dynamic responses of the two simulation models under disturbances will be compared. If they match, the calculated dynamic load model is verified to be accurate. The schematic diagram for the load model and the power grid simulation studies is shown in Fig. 3(c).

### B. VERIFICATION OF VOLTAGE DEPENDENCE

To verify the voltage dependence characteristic of the proposed dynamic load model, a remote three-phase fault is applied to the drive input, which causes a 90% voltage sag in the detailed switching model. The fault starts from 14.4 s and is cleared at 14.65 s, and the frequency of the power source remains the same. The total simulation time using Matlab/Simulink is 15 seconds.

A resultant 90% voltage sag at the drive input in the detailed switching model is applied directly to the developed dynamic load model in order to compare dynamic responses of the two models under the same voltage disturbance.

Dynamic responses of the two models for the 90% voltage sag are shown in Fig. 5. It is found that there is good agreement between the models, which verify the accuracy of the developed dynamic load model regarding the voltage dependence.

Fig. 5 shows that the real and reactive power for the medium voltage motor drive system vary significantly under a voltage disturbance. Therefore, it is not accurate to assume VFDs as constant power loads.

### C. VERIFICATION OF FREQUENCY DEPENDENCE

To verify the frequency dependence characteristic of the proposed dynamic load model, a frequency variation step-changed from 60 Hz to 55 Hz is applied at the power source in the detailed switching model. This frequency variation starts from 14.4 s and is cleared at 14.65 s. The total simulation time using Matlab/Simulink is 15 seconds.

It is interesting to note that a small voltage variation is caused by the frequency variation. Both frequency and voltage variations at the drive input in the detailed switching model are applied directly to the developed dynamic load model in order to compare dynamic responses of the two models under the same disturbances.

Dynamic responses of the two models subjected to the frequency variation are shown in Fig. 6. The comparison shows good agreement and similar tendency between the

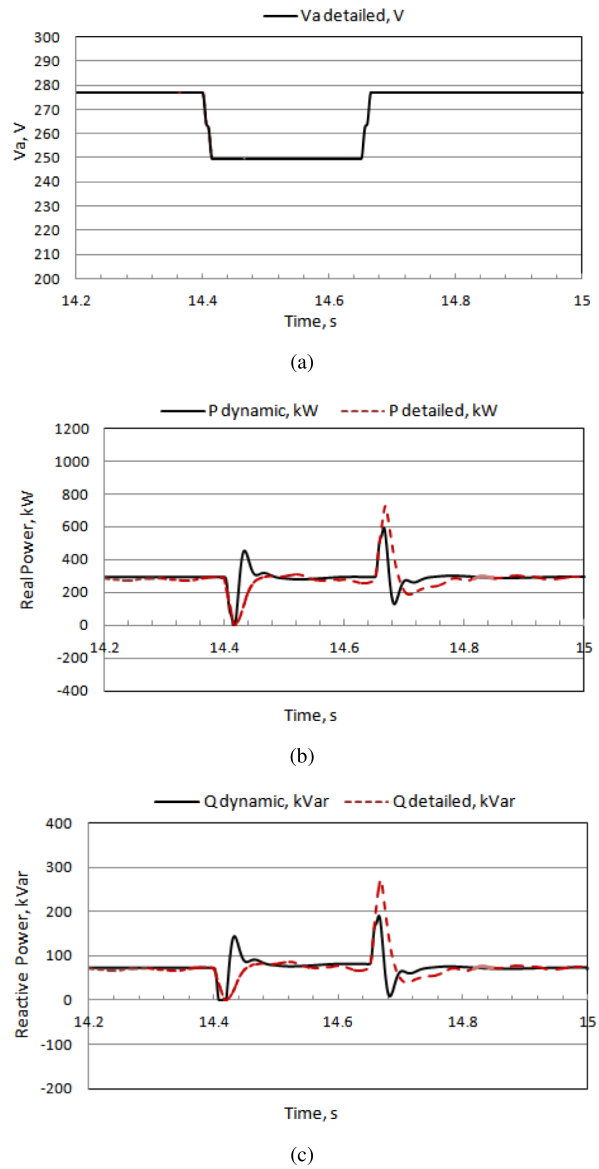


**FIGURE 5. Dynamic response of the developed dynamic load model and the detailed switching model of the sample system when subjected to a 90% voltage sag: (a) voltage sag, (b) real power P, and (c) reactive power Q.**

two models, which verifies the adequacy of the proposed model regarding the frequency dependence.

Fig. 6 indicates that the real power is not sensitive to frequency variations and almost remains the same during the frequency disturbance. However, the reactive power appears to be more sensitive to the frequency variation, and the overall reactive power is reduced to a lower value during the frequency sag.

Based on the model verification, it is concluded that the proposed dynamic load model is able to capture major dynamic characteristics of the medium voltage cascaded H-bridge multi-level inverter motor drive system and accurately determine its contribution to the power grid during

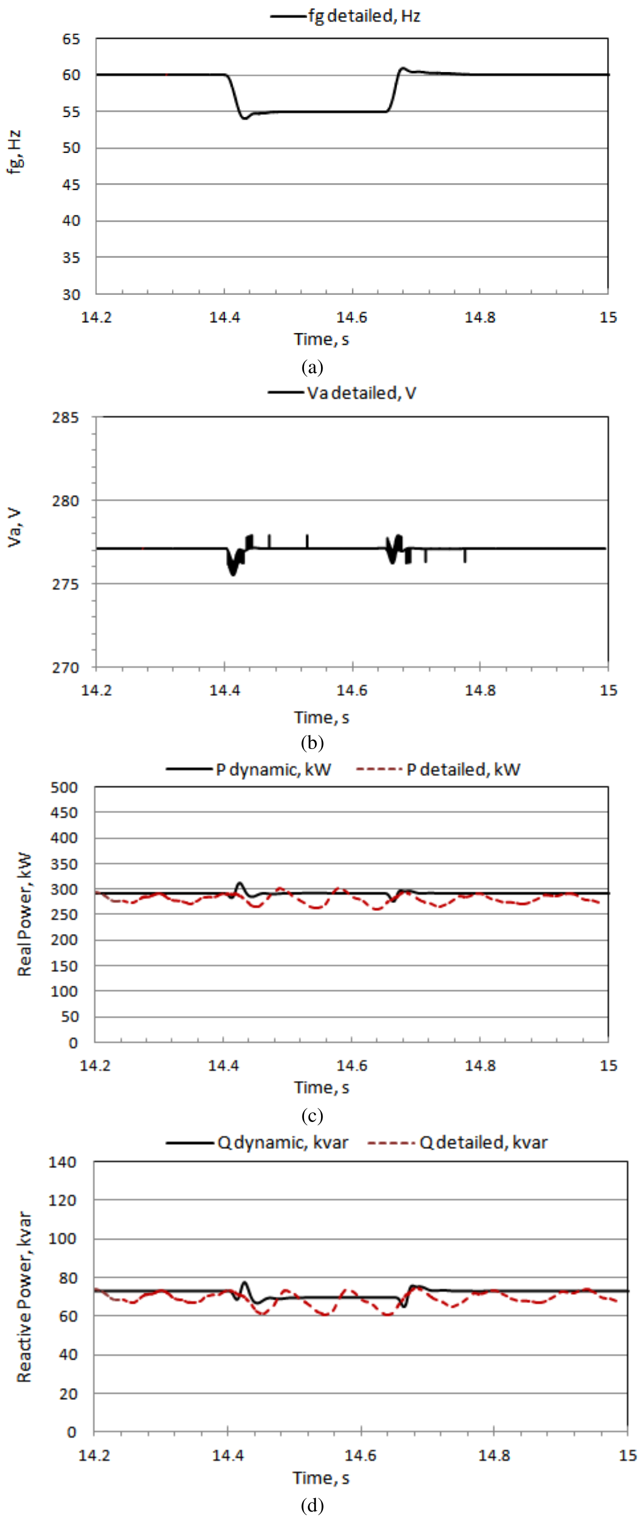


**FIGURE 6.** **Dynamic response of the developed dynamic load model and the detailed switching model for a frequency variation: (a) frequency variation, (b) voltage variation, (c) real power P, and (d) reactive power Q.**

power system disturbances. Therefore, it is an adequate model of this type of motor drive systems, and is suitable for power systems dynamic studies.

## IV. SENSITIVITY STUDY

The sensitivity study of the calculated model for the sample system in the case study is conducted to evaluate the impact of the following three parameters on dynamic response characteristics: 1) parameters of the speed *PI* controller, $K_p$ and $K_i$, for the voltage per Hz control; 2) the DC link capacitance $C_{dc}$ inside each power module of the medium voltage drive; and 3) load torque $T_L$ of the induction motor.

Fig. 7 shows the dynamic response of the calculated model for a 90% voltage sag where the parameters of the speed *PI* controller ($K_p$ and $K_i$) vary. The following three cases are

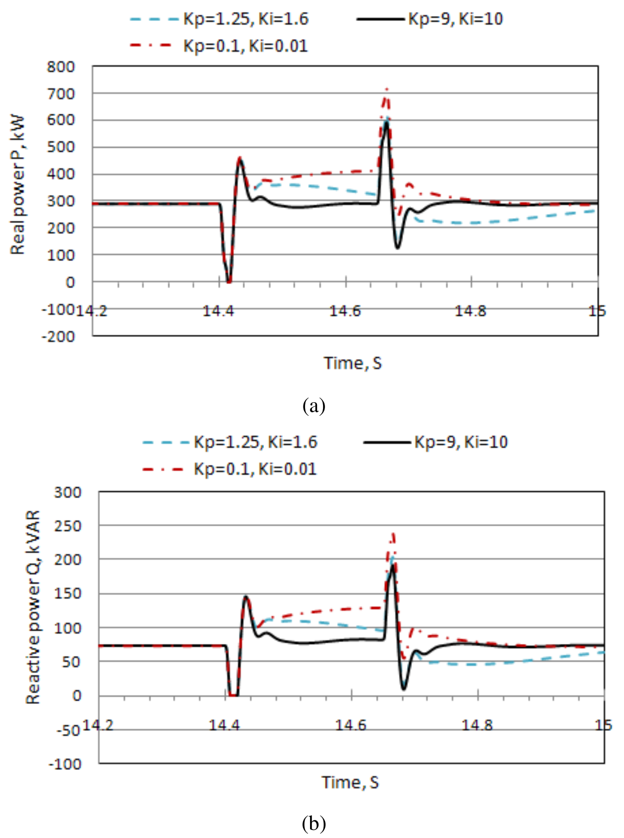


**FIGURE 7.** **Dynamic response of the developed dynamic load model due to different speed controller parameters, $K_p$ and $K_i$: (a) real power P and (b) reactive power Q.**

considered: (1) $K_p = 1.25$, and $K_i = 1.6$; (2) $K_p = 9$, and $K_i = 10$; (3) $K_p = 0.1$, and $K_i = 0.01$. Other parameters are the same as that listed in Table I. Case 2 with control parameters of $K_p = 9$ and $K_i = 10$ shows the best performance. The system is able to recover quickly after disturbances and reaches the previous steady-state values, which coincides with the detailed switching model response as shown in Fig. 5. However, Cases 1 and 3 do not have good performance during disturbances. Therefore, it is very important that proper control parameters for the speed *PI* controller are used in the calculated dynamic load model (such as $K_p = 9$ and $K_i = 10$), otherwise, the system will not be able to reach a steady-state after disturbances, and the simulation results will not match with the reality.

The simulated dynamic response of the developed model with different DC link capacitance values $C_{dc}$ inside a power module of the medium voltage drive when subjected to a 90% voltage sag are shown in Fig. 8. The $C_{dc}$ values are 9200 $\mu$F, 10000 $\mu$F and 18000 $\mu$F. Other parameters are the same as that listed in Table I. It is found that increasing the DC link capacitance tends to increase the magnitude of dynamic transient for the real and reactive power. However, it has no effect on the steady-state values for the real and reactive power.

Three different load torques $T_L$ are applied to the induction motor for the proposed dynamic model when subjected to a 90% voltage sag: 1000 Nm, 1500 Nm and 2000 Nm, which correspond to 17.3%, 25.9% and 34.5% loading of the motor, respectively. Other parameters are the same as that listed in Table I. The simulated dynamic response of the developed model in this case are shown in Fig. 9. It is found that the load factor of the motor has significant effect on both steady-state and dynamic responses for the real and reactive power.

The sensitivity study of the developed model indicates that key parameters of the motor drive system as the input data of the model calculation could have significant influence on the overall dynamic response of the model.

The practical system information and operating condition shall be used for an existing motor drive system to obtain an accurate dynamic response when creating its dynamic load model. For a system that such information is not available, the estimation as close as possible shall be made towards typical data for the system dynamic modeling.

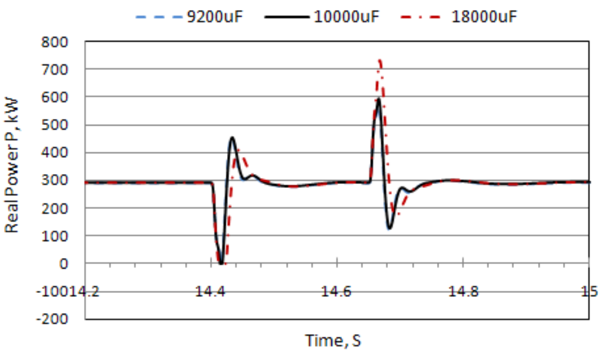


(a)

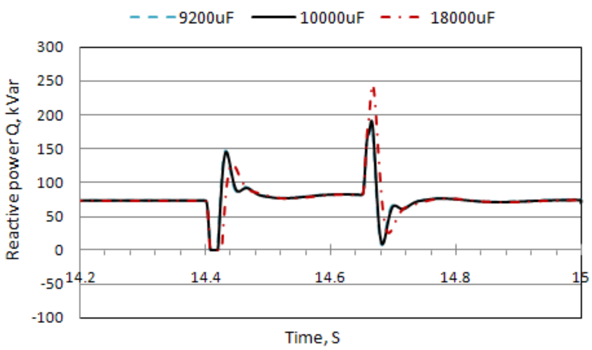


(b)

**FIGURE 8. Dynamic response of the developed dynamic model due to different DC link capacitance $C_{dc}$ of each power module inside the medium voltage drive: (a) real power P and (b) reactive power Q.**

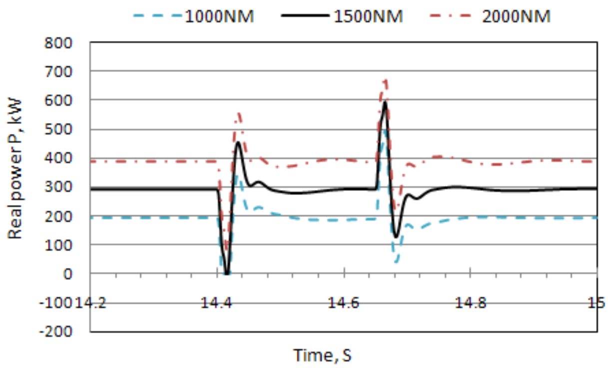


(a)

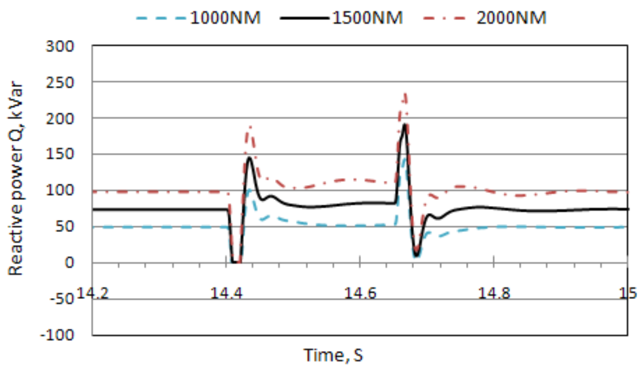


(b)

**FIGURE 9. Dynamic response of the developed dynamic model due to different load torque of the induction motor $T_L$: (a) real power P and (b) reactive power Q.**

## V. CONCLUSION

The dynamic load model for a medium voltage cascaded H-bridge multi-level PWM inverter motor drive system is developed in this paper, which is derived using an analytical method called the linearization approach. The accuracy of the proposed model is verified by a case study using a sample medium voltage motor drive system. The influence of key parameters of the model on dynamic response characteristics is evaluated through a sensitivity study.

The developed dynamic load model of the medium voltage motor drive system is expressed by 7$^{th}$ order transfer functions with both voltage and frequency dependence considered. This model can be readily inserted into large scale power system simulation software for power system dynamic studies.

## ACKNOWLEDGMENT

The authors would like to thank Dr. W. Xu with the University of Alberta for his support during the completion of this work.

## REFERENCES


[1] IEEE Task Force on Load Representation for Dynamic Performance, ''Load representation for dynamic performance analysis [of power systems],'' *IEEE Trans. Power Syst.*, vol. 8, no. 2, pp. 472–482, May 1993.

[2] IEEE Task Force on Load Representation for Dynamic Performance, ''Standard load models for power flow and dynamic performance simulation,'' *IEEE Trans. Power Syst.*, vol. 10, no. 3, pp. 1302–1313, Aug. 1995.

[3] A. Merdassi, L. Gerbaud, and S. Bacha, ''A new automatic average modelling tool for power electronics systems,'' in *Proc. IEEE Power Electron. Specialists Conf. (PESC)*, Jun. 2008, pp. 3425–3431.

[4] J. Sun and H. Grotstollen, ''Averaged modelling of switching power converters: Reformulation and theoretical basis,'' in *Proc. IEEE 23rd Annu. Power Electron. Specialists Conf. (PESC)*, vol. 2. Jun./Jul. 1992, pp. 1165–1172.

[5] S. Cuk and R. D. Middlebrook, ''A general unified approach to modelling switching-converter power stages,'' in *Proc. IEEE Annu. Power Electron. Specialists Conf. (PESC)*, Jun. 1976, pp. 18–31.

[6] A. Griffo, J. B. Wang, and D. Howe, ''State-space average modelling of 18-pulse diode rectifier,'' in *Proc. 3rd Int. Conf. Sci. Comput. Comput. Eng. (IC-SCCE)*, Jul. 2008, pp. 1–8.

[7] T. A. Meynard, M. Fadel, and N. Aouda, ''Modeling of multilevel converters,'' *IEEE Trans. Ind. Electron.*, vol. 44, no. 3, pp. 356–364, Jun. 1997.

[8] A. Uan-Zo-li, R. P. Burgos, F. Lacaux, F. Wang, and D. Boroyevich, ''Assessment of multipulse converter average models for stability studies using a quasistationary small-signal technique,'' in *Proc. 4th Int. Power Electron. Motor Control Conf.*, vol. 3. Aug. 2004, pp. 1654–1658.

[9] S. Rosado, R. Burgos, F. Wang, and D. Boroyevich, ''Large- and small-signal evaluation of average models for multi-pulse diode rectifiers,'' in *Proc. IEEE Workshops Comput. Power Electron. (COMPEL)*, Jul. 2006, pp. 89–94.

[10] A. Emadi, A. Khaligh, C. H. Rivetta, and G. A. Williamson, ''Constant power loads and negative impedance instability in automotive systems: Definition, modeling, stability, and control of power electronic converters and motor drives,'' *IEEE Trans. Veh. Technol.*, vol. 55, no. 4, pp. 1112–1125, Jul. 2006.

[11] P. C. Krause, O. Wasynczuk, and S. D. Sudhoff, *Analysis of Electric Machinery and Drive Systems*, 2nd ed. Piscataway, NJ, USA: IEEE Press, 2002.

[12] S. A. Y. Sabir and D. C. Lee, ''Dynamic load models derived from date acquired during system transients,'' *IEEE Trans. Power App. Syst.*, vol. PAS-101, no. 9, pp. 3365–3372, Sep. 1982.

[13] T. Omata and K. Uemura, ''Effects of series impedance on power system load dynamics,'' *IEEE Trans. Power Syst.*, vol. 14, no. 3, pp. 1070–1077, Aug. 1999.

[14] F. T. Dai, J. V. Milanovic, N. Jenkins, and V. Roberts, ''Development of a dynamic power system load model,'' in *Proc. 7th Int. Conf. AC-DC Power Transmiss.*, Nov. 2001, pp. 344–349.

[15] X. Liang and W. Xu, ''Modeling variable frequency drive and motor systems in power systems dynamic studies,'' in *Proc. IEEE Ind. Appl. Soc. (IAS) Annu. Meeting*, Oct. 2013, pp. 1–11.

[16] X. Liang, ''Linearization approach for modeling power electronics devices in power systems,'' *IEEE J. Emerg. Sel. Topics Power Electron.*, vol. 2, no. 4, pp. 1003–1012, Dec. 2014.

[17] P. W. Hammond, ''A new approach to enhance power quality for medium voltage AC drives,'' *IEEE Trans. Ind. Appl.*, vol. 33, no. 1, pp. 202–208, Jan./Feb. 1997.

[18] W. A. Hill and C. D. Harbourt, ''Performance of medium voltage multilevel inverters,'' in *Proc. 34th IEEE Ind. Appl. Soc. (IAS) Annu. Meeting*, vol. 2. Oct. 1999, pp. 1186–1192.

[19] P. W. Hammond, ''Enhancing the reliability of modular medium-voltage drives,'' *IEEE Trans. Ind. Electron.*, vol. 49, no. 5, pp. 948–954, Oct. 2002.

[20] Y. Fukuta and G. Venkataramanan, ''DC bus ripple minimization in cascaded H-bridge multilevel converters under staircase modulation,'' in *Proc. 37th IEEE Ind. Appl. Soc. (IAS) Annu. Meeting*, vol. 3. Oct. 2002, pp. 1988–1993.

[21] M. Rastogi and P. W. Hammond, ''Dual-frequency braking in AC drives,'' *IEEE Trans. Power Electron.*, vol. 17, no. 6, pp. 1032–1040, Nov. 2002.

[22] G. J. Rogers, J. Di Manno, and R. T. H. Alden, ''An aggregate induction motor model for industrial plants,'' *IEEE Trans. Power App. Syst.*, vol. PAS-103, no. 4, pp. 683–690, Apr. 1984.

[23] P. Kundur, *Power System Stability and Control*. New York, NY, USA: McGraw-Hill, 1994.



**XIAODONG LIANG** (M'06–SM'09) received the B.Eng. and M.Eng. degrees from Shenyang Polytechnic University, Shenyang, China, in 1992 and 1995, respectively, the M.Sc. degree from the University of Saskatchewan, Saskatoon, Canada, in 2004, and the Ph.D. degree from the University of Alberta, Edmonton, Canada, in 2013, all in electrical engineering.

She served as a Lecturer with Northeastern University, Shenyang, from 1995 to 1999. In 2001, she joined Schlumberger, Edmonton, AB, Canada. She was a Principal Power Systems Engineer with Schlumberger before joining Washington State University, Vancouver, WA, USA, in 2013. From 2013 to 2015, she was an Assistant Professor with Washington State University. In 2015, she joined the Memorial University of Newfoundland, St. John's, NL, Canada, where she is currently an Assistant Professor. Her research interests include power system dynamics, power quality, and electric machines.

Dr. Liang is a Registered Professional Engineer in the Provinces of Alberta and Newfoundland and Labrador Canada.



**JINWEI HE** received the B.Eng. degree from Southeast University, Nanjing, China, in 2005, the M.Sc. degree from the Institute of Electrical Engineering, Chinese Academy of Sciences, in 2008, and the Ph.D. degree from the University of Alberta, Canada, in 2013, all in electrical engineering.

From 2008 to 2009, he was an Electrical Design Engineer with the China Electronics Technology Group Corporation, Beijing, China. In 2012, he was a Visiting Scholar with Aalborg University, Aalborg, Denmark. He has been a Power Electronics Engineer with Accuenergy Canada, North York, ON, Canada, since 2013. He joined Tianjin University, Tianjin, China, in August 2015. His research interests include variable frequency drive of linear electric machine, high power electronics applications in distributed power generation and ground transportation, and linear eclectic machine electromagnetic design.